King Fahd University of Petroleum & Minerals

DEPARTMENT OF MATHEMATICAL SCIENCES

Technical Report Series

TR 271

January 2002

Initial Inverse Problem in Heat Equation with Bessel Operator

Khalid Masood, Salim Messaoudi, F.D. Zaman

DHAHRAN 31261 ● SAUDI ARABIA ● www.kfupm.edu.sa/math/ ● E-mail: mathdept@kfupm.edu.sa

INITIAL INVERSE PROBLEM IN HEAT EQUATION WITH BESSEL OPERATOR

Khalid Masood, Salim Messaoudi and F. D. Zaman
Department of Mathematical Sciences
King Fahd University of Petroleum and Minerals
Dhahran 31261, Saudi Arabia
masood@kfupm.edu.sa

Abstract

We investigate the inverse problem involving recovery of initial temperature from the information of final temperature profile in a disc. This inverse problem arises when experimental measurements are taken at any given time, and it is desired to calculate the initial profile. We consider the usual heat equation and the hyperbolic heat equation with Bessel operator. An integral representation for the problem is found, from which a formula for initial temperature is derived using Picard's criterion and the singular system of the associated operators.

1. Introduction

Initial inverse problems are much less encountered in the literature than the other type of inverse problems. The reason is that the initial condition influences the temperature distribution inside a body only for a limited time on account of the classical Fourier-Kirchhoff law that assumes the infinite velocity of heat waves. Also, the initial inverse problem based on the parabolic heat equation is extremely ill-posed; see e.g. Engl [1]. There is another approach to this inverse problem that consists of a complete reformulation of the governing equation. The inverse problem based upon the parabolic heat equation is closely approximated by a hyperbolic heat equation; see e.g. Weber[2], and Elden[3]. This alternate formulation gives rise to an inverse problem, which is stable and well-posed and thus gives more reliable results. Moreover, as we see later, the parabolic heat conduction model can be treated as a limiting case of the hyperbolic model.

The need to consider the alternate formulation has some physical advantages. In many applications, one encounters a situation where the usual parabolic heat equation does not serve as a realistic model. Since the speed of propagation of the thermal signal is finite, e.g. for short-pulse laser applications, the hyperbolic differential equation correctly models the problem; see Vedavarz et al. [4] and Gratzke et al. [5] among others. We present here an inverse problem which seeks the initial temperature distribution from a given final temperature in a disc using a parabolic as well as a hyperbolic model.

In this paper we are concerned with the study of radially symmetric solutions in a disc. The heat equation with Bessel operator possess radially symmetric solutions in a disc, see for instance Wyld [6] and Walter [7]. We will consider the hyperbolic heat equation with a small parameter and we will show that its solution approximates the solution to the parabolic heat equation. The initial inverse problem in the hyperbolic heat equation is stable and well posed. Moreover, numerical methods for hyperbolic problems are efficient and accurate. We will utilize the small value of the parameter and apply the WKBJ method to solve the initial inverse problem, see Bender and Orszag [8]. We will also show that by controlling the size of the parameter the solution may give some information for higher modes in case there is white Gaussian noise added to the data. In the second section we will solve the inverse problem by considering the heat equation with Bessel operator. In the third section the inverse problem in the hyperbolic equation with a small parameter will be solved and compared with the inverse solution of the heat equation. An example will also be presented to check the validity of the inverse solution. We will perform some numerical experiments and the results of these experiments will be analyzed in the fourth section. Finally in the last section the results will be summarized.

2. Initial inverse problem in the heat equation

We consider

$$\frac{\partial u}{\partial t} = \frac{\partial^2 u}{\partial x^2} + \frac{1}{x}\frac{\partial u}{\partial x}, \qquad 0 < x < 1, \tag{1}$$

with zero temperature at one boundary

$$u(1,t) = 0, \tag{2}$$

and assume the final temperature distribution

$$f(x) = u(x,T)\,. \tag{3}$$

We want to recover the initial temperature profile

$$g(x) = u(x,0)\,. \tag{4}$$

The boundary condition (2) can be replaced by an insulated boundary, i.e. $u_x(1,t) = 0$, because it is important in some applications. All details for insulated boundary condition can be carried out in a similar manner to that described in this paper.

We assume by separation of variables, solution of the direct problem of the form

$$u(x,t) = \sum_{n=1}^{\infty} v_n(t)\,\phi_n(x)\,, \tag{5}$$

The corresponding eigenvalue problem is given by

$$\frac{d}{dx}\left[x\frac{d\phi(x)}{dx}\right] + \lambda x\phi(x) = 0, \qquad 0 < x < 1, \tag{6}$$

together with

$$\phi(1) = 0. \tag{7}$$

At the singular end point $x = 0$, from the application point of view, we impose a boundary condition of the form

$$\lim_{x \to 0} x\frac{d\phi(x)}{dx} = 0. \tag{8}$$

In application to heat conduction problems, x is the radial cylindrical coordinate and condition (8) states that total heat flux through a small circle surrounding the origin vanishes, that is, there is no heat source at the origin. The independent solutions of (6) for $\lambda \neq 0$ are $J_0\left(\sqrt{\lambda}x\right)$ and $N_0\left(\sqrt{\lambda}x\right)$. But from these two independent solutions only $J_0\left(\sqrt{\lambda}x\right)$ satisfies (8). It is usual to replace (8) by the condition that the solution be finite at the origin, which has the same effect as far as selecting $J_0\left(\sqrt{\lambda}x\right)$ as the only admissible solution. Now we apply condition (7), which gives rise to a sequence $\{\lambda_n\}$ of positive eigenvalues and the corresponding eigenfunctions are $J_0\left(\sqrt{\lambda_n}x\right)$. These eigenfunctions are orthogonal in the Hilbert space $H_x[0,1]$, where x is the weight function. These eigenfunctions can be normalised to give

$$\phi_n(x) = \frac{\sqrt{2}}{J_0'\left(\sqrt{\lambda_n}\right)} J_0\left(\sqrt{\lambda_n}x\right), \tag{9}$$

where $'$ denotes derivative with respect to x.

The eigenfunctions given by (9) are complete in $H_x[0,1]$, and therefore $g(x) \in H_x[0,1]$ can be expanded as

$$g(x) = \sum_{n=1}^{\infty} c_n\phi_n(x), \tag{10}$$

where

$$c_n = \int_0^1 \zeta \phi_n(\zeta)\, g(\zeta)\, d\zeta. \tag{11}$$

Now by using (5), $v_n(t)$ satisfies the following initial value problem

$$\frac{dv_n(t)}{dt} = -\lambda_n v_n(t)\,, \tag{12}$$

$$v_n(0) = c_n, \tag{13}$$

where we have used the following relation

$$\int_0^1 x\phi_n'(x)\, \phi_m'(x)\, dx = \begin{cases} 0 & m \neq n \\ \lambda_n & m = n \end{cases}. \tag{14}$$

So, we can write the solution of the direct problem (1) in the form

$$u(x,t) = \sum_{n=1}^{\infty} c_n \exp[-\lambda_n t]\, \phi_n(x)\,. \tag{15}$$

This represents an analytical solution to the heat equation in cylindrical coordinates, see Carslaw and Jaeger [9]. Now by applying (3), we can write

$$f(x) = \int_0^1 K(x,\zeta)\, g(\zeta)\, d\zeta, \tag{16}$$

where

$$K(x,\zeta) = \sum_{n=1}^{\infty} \zeta \exp[-\lambda_n T]\, \phi_n(\zeta)\, \phi_n(x)\,. \tag{17}$$

Thus the inverse problem is reduced to solving integral equation of the first kind. The singular system of the integral operator in (16) is

$$\{\exp[-\lambda_n T]\,;\ \phi_n(x)\,,\ \phi_n(x)\} \tag{18}$$

Now by application of Picard's theorem (see Engl [1]) the inverse problem is solvable iff

$$\sum_{n=1}^{\infty} \exp[2\lambda_n T] \left| f_n \right|^2 < \infty, \tag{19}$$

where

$$f_n = \int_0^1 \zeta \phi_n(\zeta) \, f(\zeta) \, d\zeta, \tag{20}$$

are the classical Fourier coefficients of f. Now again by Picard's theorem, we can recover the initial profile by the following expression

$$g\left(x\right) = \sum_{n=1}^{\infty} \exp\left[\lambda_n T\right] f_n \phi_n\left(x\right). \tag{21}$$

Picard's theorem demonstrates the ill-posed nature of the problem considered. If we perturb the data by setting $f^\delta = f + \delta\phi_n$ we obtain a perturbed solution $g^\delta = g + \delta\phi_n \exp[\lambda_n T]$. Hence the ratio $\left\|g^\delta - g\right\| / \left\|f^\delta - f\right\| = \exp[\lambda_n T]$ can be made arbitrarily large due to the fact that the singular values $\exp[-\lambda_n T]$ decay exponentially, see Fig. 1. The influence of errors in the data f is obviously controlled by the rate of this decay. This error can also be controlled further by choosing a small value of T, for example for $T = 1$, a small error in the n-th Fourier coefficient is amplified by the factor $\exp[\lambda_n]$. So to regularize, we confine ourselves to lower modes by only retaining the first few terms in the series (21). This technique of truncating the series is known as truncated singular value decomposition (TSVD), see Hansen [10]. Also see [10], for a method of choosing the appropriate number of terms in the series.

3. Initial inverse problem in the hyperbolic heat equation

There is an alternate approach to the heat conduction problem [2,3], which consists of introducing a hyperbolic term with a small parameter. By controlling the size of

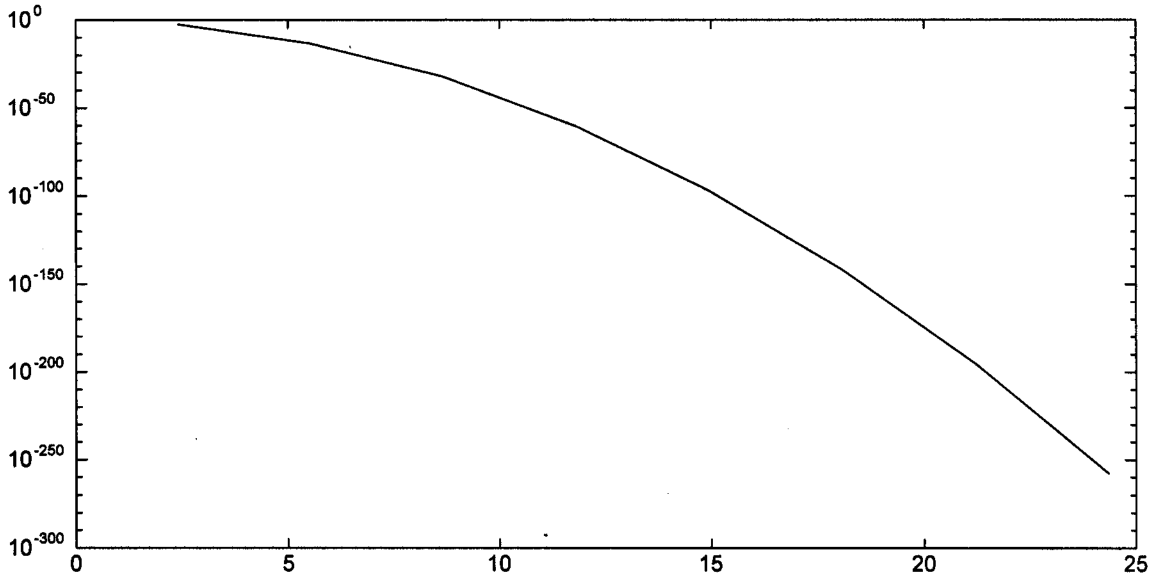

FIG. 1. First 100 singular values for $T = 1$ on a log-scale.

the parameter we would like to obtain an approximate solution to the heat conduction problem. Also in some interesting situations the coefficient of the term $\frac{\partial^2 u}{\partial t^2}$ is small due to properties of the material [4,5]. So, we reformulate the problem as follows:

$$\epsilon \frac{\partial^2 u}{\partial t^2} + \frac{\partial u}{\partial t} = \frac{\partial^2 u}{\partial x^2} + \frac{1}{x}\frac{\partial u}{\partial x}, \quad 0 < x < 1, \tag{22}$$

together with $(2)-(4)$ and (8) and $\epsilon \to 0^+$. We impose one more condition as follows:

$$\frac{\partial u}{\partial t}(x,0) = 0. \tag{23}$$

As before, by separation of variables, we assume solution of the form (5). In this case $v(t)$ has to solve the following initial value problem

$$\epsilon \frac{d^2 v_n(t)}{dt^2} + \frac{d v_n(t)}{dt} = -\lambda_n v_n(t)\,, \tag{24}$$

$$v_n(0) = c_n, \tag{25}$$

$$\frac{dv_n(0)}{dt} = 0. \tag{26}$$

Since $\epsilon \to 0^+$, this is a singular perturbation problem. We apply the WKBJ method to obtain an asymptotic representation for the solution of (24) containing parameter ϵ; the representation is to be valid for small values of the parameter. It is demonstrated in [8] that the solution stays closer to the exact solution for large values such as $\epsilon = 0.5$. The solution of (24) is given by

$$v_n(t) = \left(\frac{\epsilon\lambda_n - 1}{2\epsilon\lambda_n - 1}\right) c_n \exp[-\lambda_n t] + \left(\frac{\epsilon\lambda_n c_n}{2\epsilon\lambda_n - 1}\right) \exp\left[\lambda_n t - \frac{t}{\epsilon}\right]. \tag{27}$$

As before, we can use this solution in (5) to arrive at an integral equation of the form (16). The singular system in this case is

$$\left\{\left(\frac{\epsilon\lambda_n - 1}{2\epsilon\lambda_n - 1}\right) \exp[-\lambda_n T] + \left(\frac{\epsilon\lambda_n}{2\epsilon\lambda_n - 1}\right) \exp\left[\lambda_n T - \frac{T}{\epsilon}\right];\ \phi_n(x),\ \phi_n(x)\right\} \tag{28}$$

Now by Picard's theorem (see Engl[1]) the solution exists iff

$$\sum_{n=1}^{\infty} \frac{|f_n|^2}{\left[\left(\frac{\epsilon\lambda_n - 1}{2\epsilon\lambda_n - 1}\right) \exp[-\lambda_n T] + \left(\frac{\epsilon\lambda_n}{2\epsilon\lambda_n - 1}\right) \exp\left[\lambda_n T - \frac{T}{\epsilon}\right]\right]^2} < \infty, \tag{29}$$

where the Fourier coefficients f_n are given by (20). The initial profile can be recovered by the following expression

$$g(x) = \sum_{n=1}^{\infty} \frac{\phi_n(x)}{\left[\left(\frac{\epsilon\lambda_n - 1}{2\epsilon\lambda_n - 1}\right) \exp[-\lambda_n T] + \left(\frac{\epsilon\lambda_n}{2\epsilon\lambda_n - 1}\right) \exp\left[\lambda_n T - \frac{T}{\epsilon}\right]\right]}. \tag{30}$$

The solution given by (19) and (21) can be recovered by letting $\epsilon \to 0^+$ in equation (29) and (30) respectively.

Since the non-linear operators do not have singular values and singular functions; we cannot apply the method to non-linear equations. For example for the nonlinear heat equation, $u_t = (\kappa(u)u_x)_x$, the method of approximating it with the hyperbolic model presented in this section still works but the method of singular value decomposition does not.

Example: Let us consider an initial temperature distribution of the form

$$g(x) = \frac{\sqrt{2}}{J_0'\left(\sqrt{\lambda_m}\right)} J_0\left(\sqrt{\lambda_m} x\right). \tag{31}$$

First we solve the direct problems (1) and (22) together with conditions (2) – (4), (8) and (23), to find the final profiles . The Fourier coefficients corresponding to the final profiles of the parabolic and hyperbolic models respectively are

$$f_m = \exp[-\lambda_m T], \tag{32}$$

$$f_m = \left(\frac{\epsilon\lambda_m - 1}{2\epsilon\lambda_m - 1}\right) \exp[-\lambda_m T] + \left(\frac{\epsilon\lambda_m}{2\epsilon\lambda_m - 1}\right) \exp\left[\lambda_m T - \frac{T}{\epsilon}\right]. \tag{33}$$

Now we use the Fourier coefficients given by (32) and (33) in (21) and (30) respectively to recover the initial profile. It is clear that in both cases the recovered initial profile is (31).

4. Numerical experiments

Now we use the final data for the hyperbolic heat equation given by (33) in the parabolic model (21) and compare it with the exact initial profile for different values of the parameter. Also, we use the final data for the parabolic heat equation given by (32) in the hyperbolic model (30) and compare it with the exact initial profile. We consider the initial profile given by (31) for $m = 2$, also setting $T = 1$. Then we add white Gaussian noise in the data (32) and use it in the model (21) and (30)

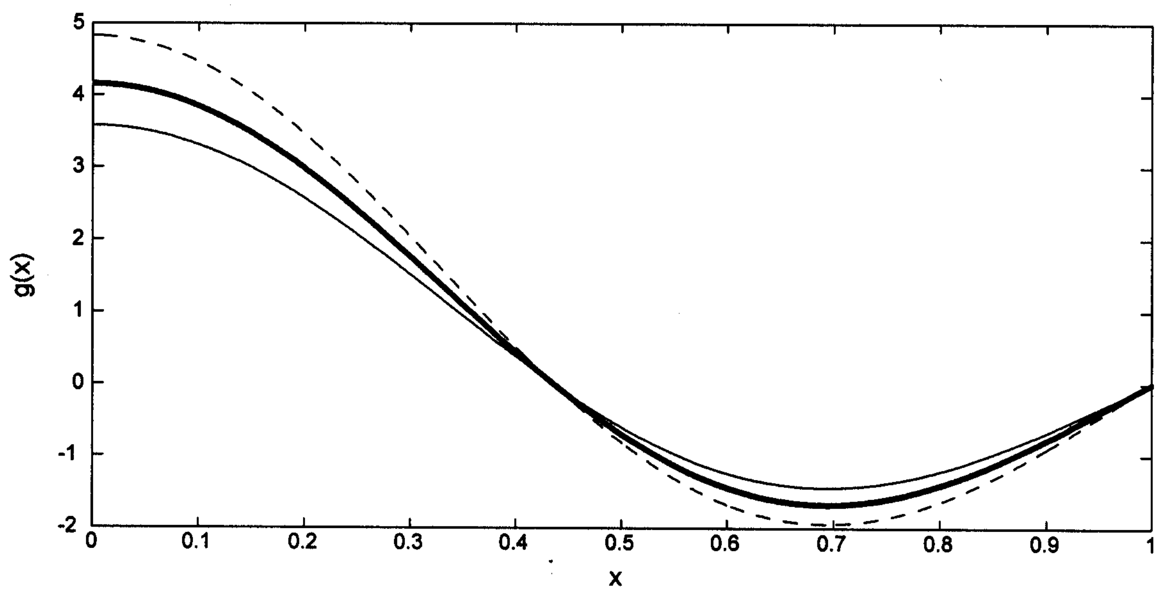

FIG. 2. The case $m = 2, T = 1, \epsilon = 0.004$.

and compare it with the exact initial profile for different values of the parameter ϵ. We also consider the higher modes and see its effects on recovery of initial profile by using noisy data.

In Figs. 2-3, the thick solid line represents the exact initial profile, the thin solid line and dotted line for the initial profile when (32) and (33) are used in (30) and (21) respectively.

It is evident from Figs. 2-3, that the solution of the hyperbolic model closely approximates the heat conduction model. It approaches the exact profile as $\epsilon \longrightarrow 0^+$. Furthermore, it approaches to the exact profile from below, so it is stable.

Now we analyze the models by adding white Gaussian noise to the data. In Figs. 4-9, we use the noisy data in both parabolic and hyperbolic models and see the mean behaviour of 100 independent realizations. The noisy data used in the heat equation model (21) is represented by a dotted line and in the hyperbolic model (30) by a thin solid line and the exact initial profile by a thick solid line.

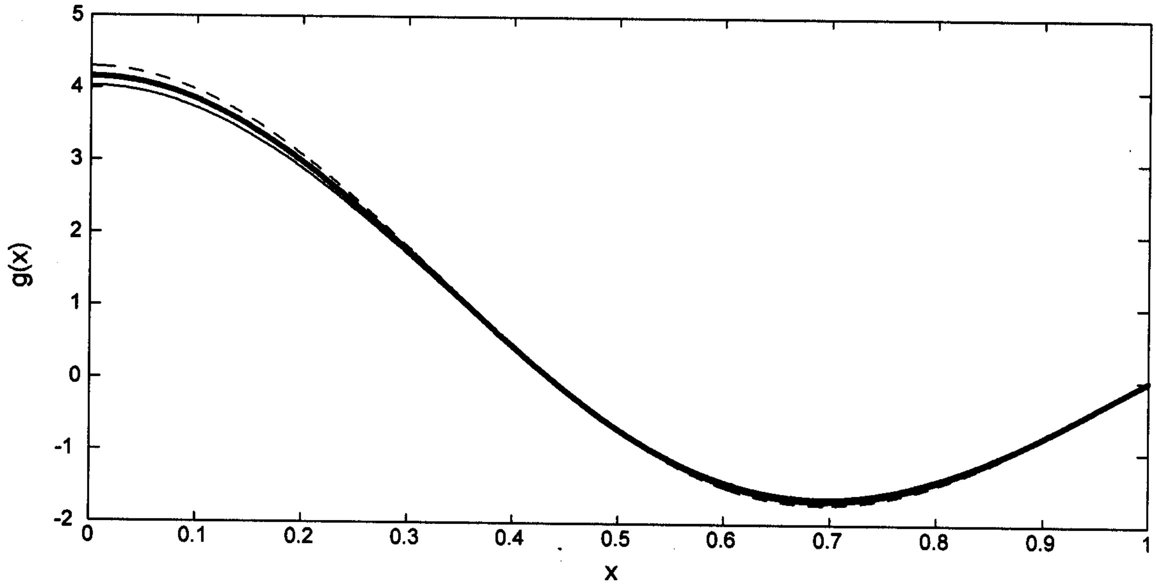

FIG. 3. The case $m = 2, T = 1$, $\epsilon = 0.001$.

We have considered the second mode, that is, $m = 2$ in Figs. 4-6 . Also we have retained first three terms ($N = 3$) in series (21) and (30). In Fig. 4, the signal to noise ratio (SNR) is equal to 620 dB (we have chosen SNR=620 dB to ensure that both the models appear clearly in the Figure) and $\epsilon = 0.003$. The hyperbolic model behaves better than the parabolic model even for this low level of noise. We have increased the level of noise in Figs. 5-6 to SNR=30 dB. In Fig. 6, the approximation of exact initial profile by the hyperbolic model is demonstrated with an appropriate choice of ϵ. How to choose ϵ is discussed in the last paragraph of this section. The inherent instability of the parabolic model is clear from Fig. 5 by noting that the vertical axis is of order 10^{30}.

In Figs. 7-9, we have considered $m = 4$ and $N = 4$. In Fig. 7, we set SNR=1160 dB, $\epsilon = 0.002$, and see the effects of this very low noise on both the models as compared to the exact profile. We increase SNR to 30 dB and observe the behaviour of the parabolic model in Fig. 8, noting that the vertical axis is given in units of

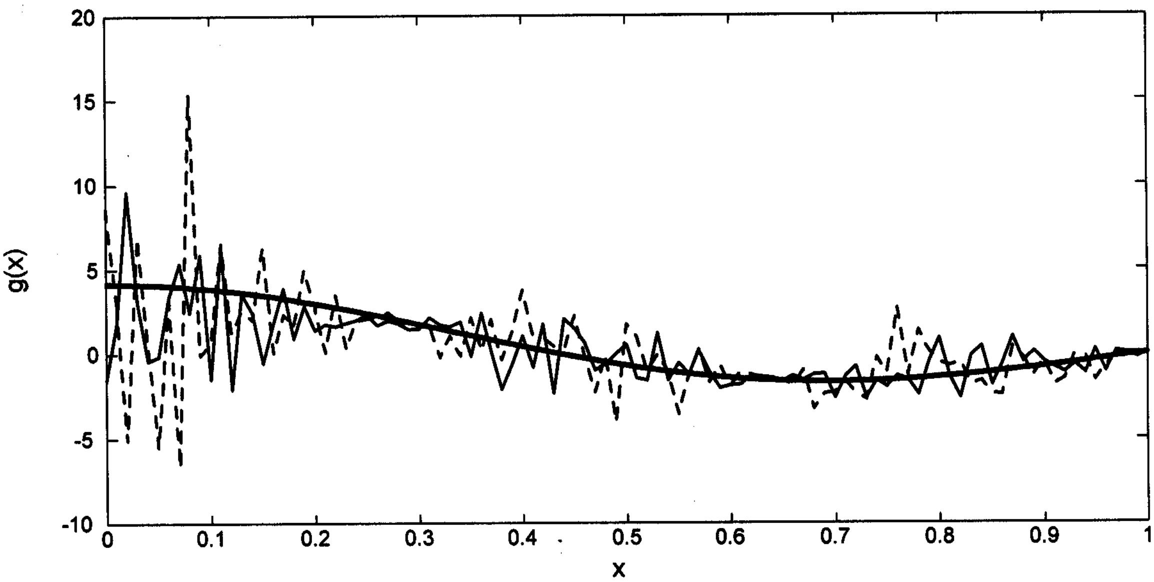

FIG. 4. The case of noisy data with SNR=620 dB, $N = 3$, $m = 2, T = 1$, $\epsilon = 0.003$.

10^{58}. However for the hyperbolic model in Fig. 9 with SNR=30 dB and $\epsilon = 0.027$, some information of the initial profile may be recovered. So, from the above analysis of figures, we conclude that the hyperbolic model behaves much better than the parabolic model in the case of noisy data. Even for lower modes, if the magnitude of noise increases, the parabolic model becomes highly unstable.

To see the effects of the size of parameter T in both models, we set $T = 2$ in Figs. 11-13. Comparing Figs. 11-12 with Figs. 5-6 and Figs. 13-14 with Figs. 8-9. For the parabolic model, the error is more than double. However for the hyperbolic model, there is very little degradation.

To choose ϵ, we start from a higher value of ϵ for which there is no signal appearing on the graph. We gradually reduce the size and note the values of ϵ for which the signal starts to appear. We reduce the size further and note the values of ϵ for which the signal amplifies significantly. Then we take the mean of the two values of ϵ, which will give an appropriate choice of ϵ. For example, in Fig. 9, the signal

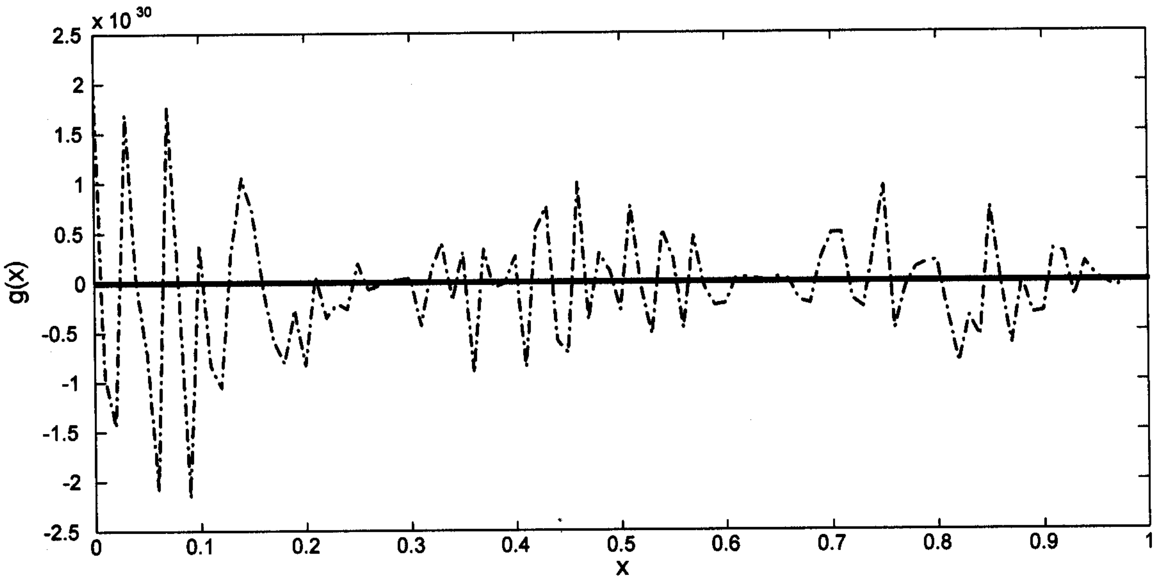

FIG. 5. The case of noisy data with SNR=30 dB, $N = 3, T = 1$, $m = 2$.

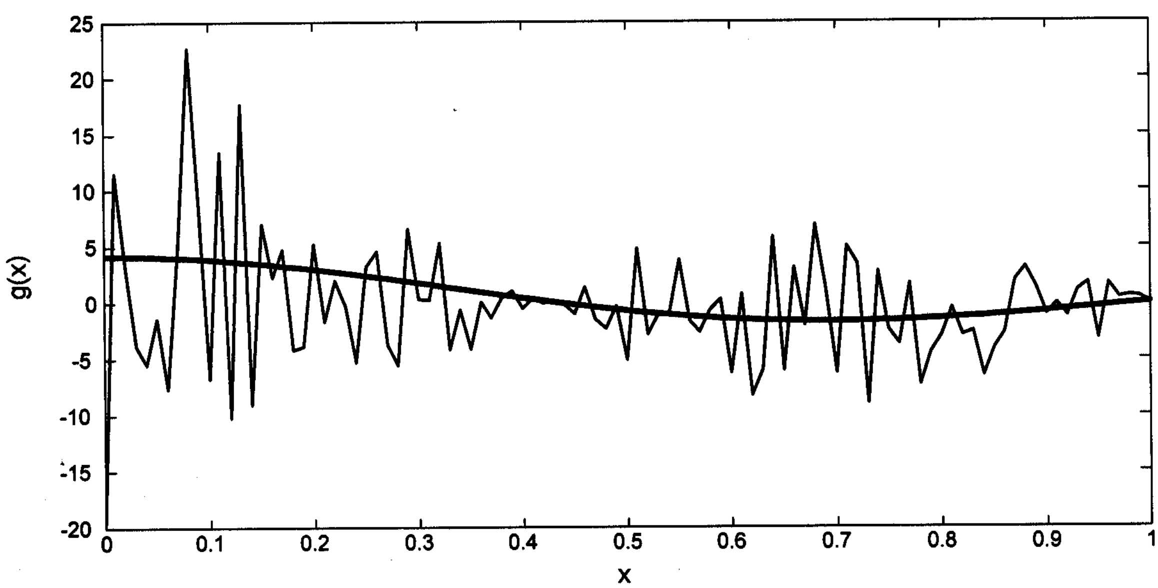

FIG. 6. The case of noisy data with SNR=30 dB, $N = 3$, $m = 2, T = 1$, $\epsilon = 0.0275$.

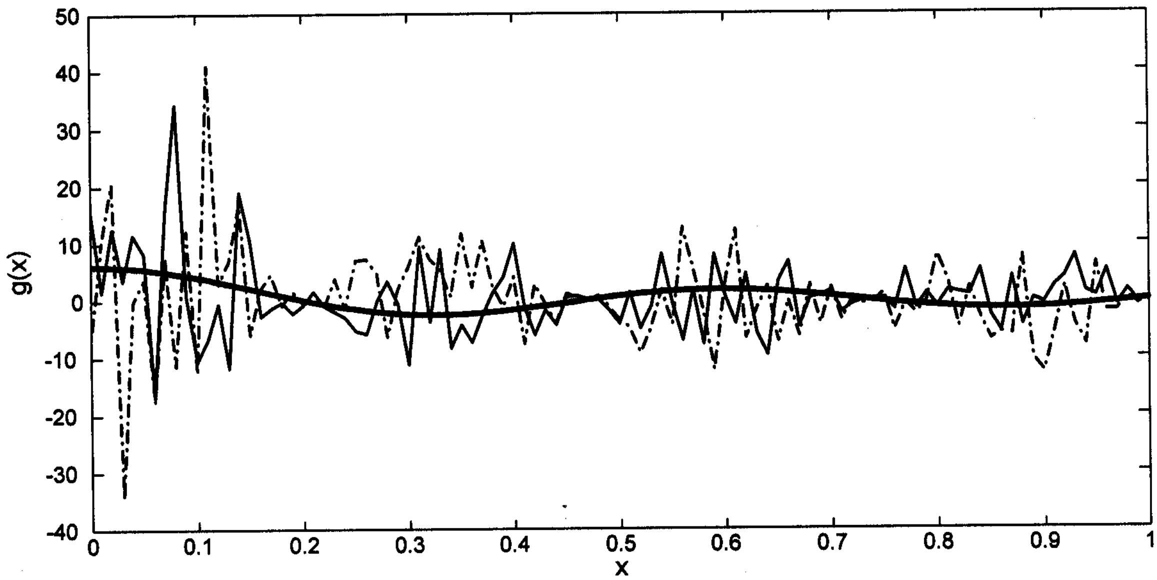

FIG. 7. The case of noisy data with SNR=1160 dB, $N = 4, T = 1$, $m = 4$, $\epsilon = 0.002$.

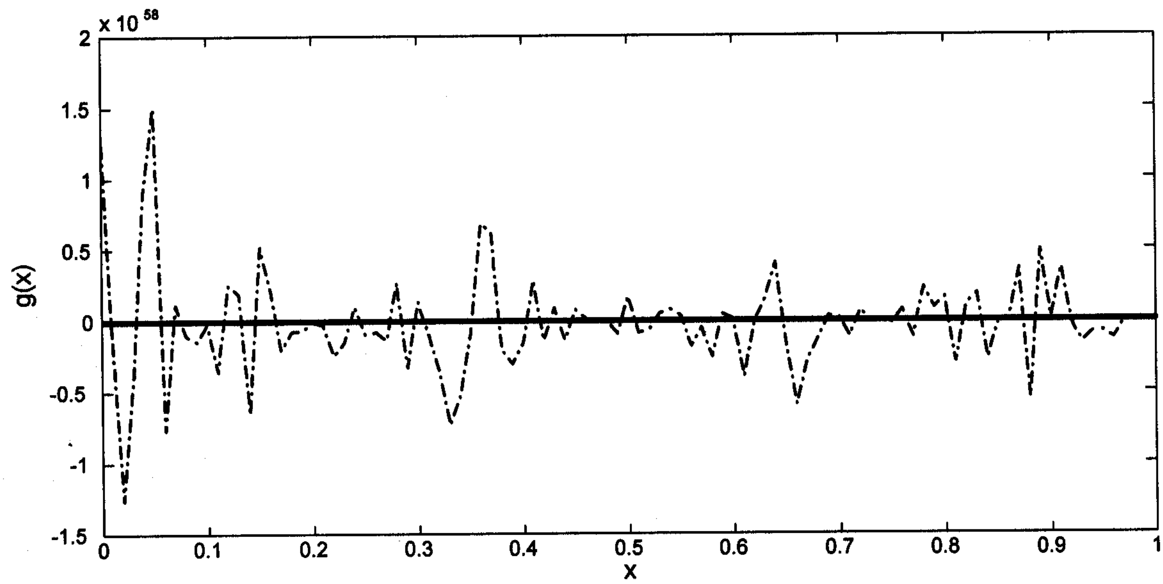

FIG. 8. The case of noisy data with SNR=30 dB, $N = 4, T = 1$, $m = 4$.

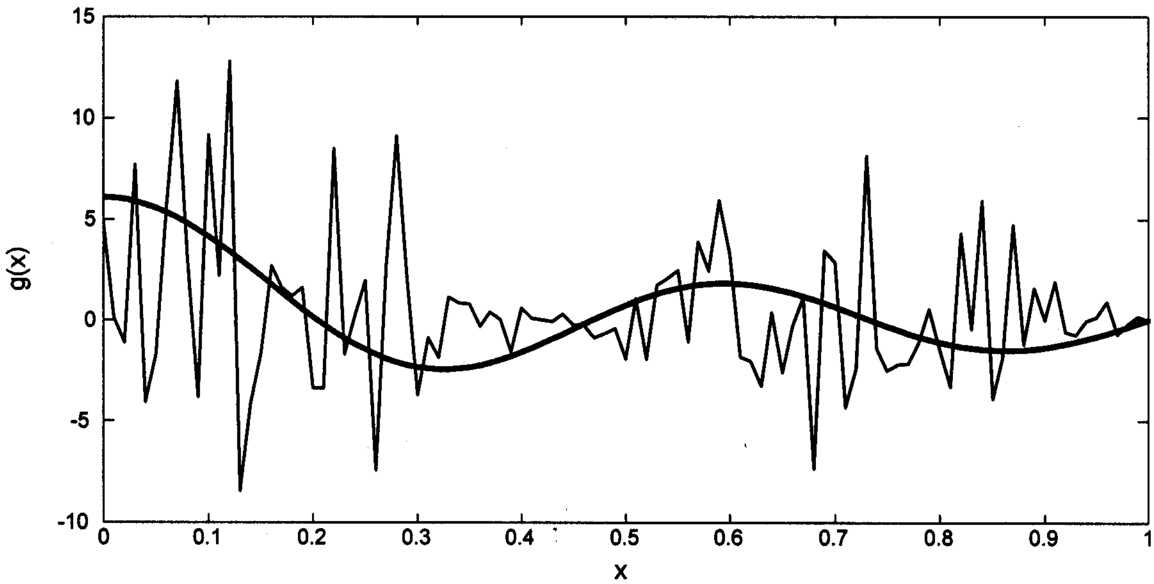

FIG. 9. The case of noisy data with SNR=30 dB, $m = 4, T = 1$, $\epsilon = 0.027$.

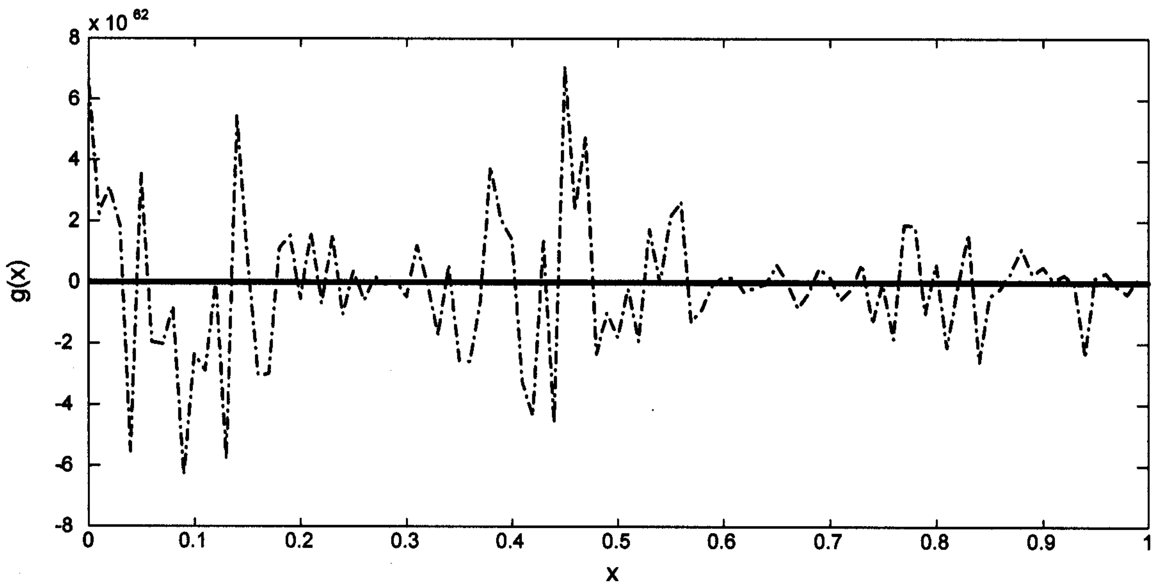

FIG. 10. The case of noisy data with SNR=30 dB, $N = 3, T = 2$, $m = 2$.

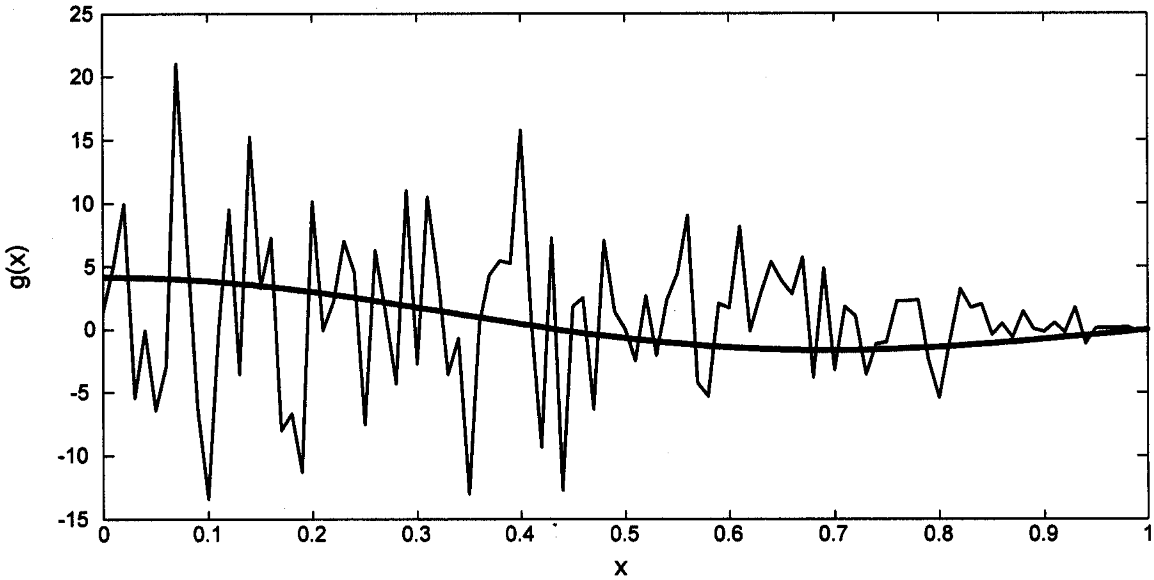

FIG. 11. The case of noisy data with SNR=30 dB, $N = 3, T = 2$, $m = 2, \epsilon = 0.1$.

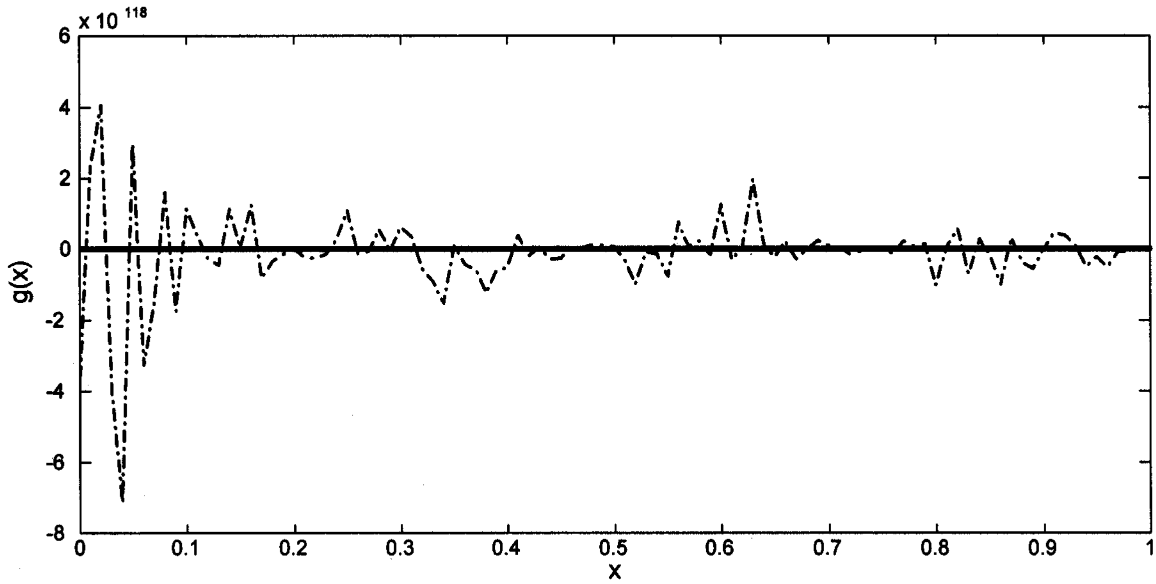

FIG. 12. The case of noisy data with SNR=30 dB, $N = 4, T = 2$, $m = 4$.

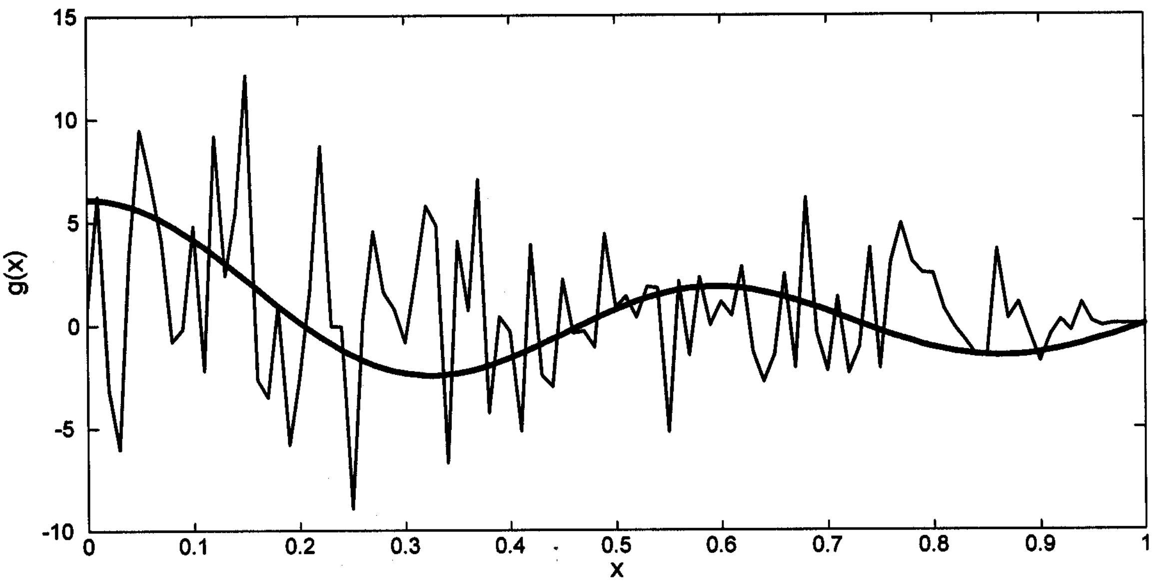

FIG. 13. The case of noisy data with SNR=30 dB, $N = 4, T = 2$, $m = 4, \epsilon = 0.1$.

starts to appear for $\epsilon = 0.03$ and amplifies to a significant level for $\epsilon = 0.0024$. So the appropriate choice of ϵ is approximately 0.0027 and it may be refined further by checking neighbouring values of 0.0027 for which the spikes are milder. We have observed that the same procedure of finding ϵ works for higher modes as well as for lower modes.

5. Conclusions

The inverse solution of the heat conduction model is characterized by discontinuous dependence on the data. A small error in the nth Fourier coefficient is amplified by the factor $\exp[\lambda_n T]$. Thus it depends on the rate of decay of singular values and this rate of decay also depends on the size of the parameter T. In order to get some meaningful information, one has to consider first few degrees of freedom in the data and has to filter out everything else depending on the rate of decay of singular values and the size of parameter T.

It is shown that a complete reformulation of the heat conduction problem as a hyperbolic equation produces meaningful results. The hyperbolic model with a small parameter closely approximates the heat conduction equation. It is also shown that in case of noisy data, the hyperbolic model approximates the exact initial profile better than the parabolic heat conduction model. Further, in the case of noisy data, the information about the initial profile cannot even be recovered for higher modes by the parabolic heat conduction model but the hyperbolic model may give some useful information about the initial profile if the value of parameter ϵ is chosen appropriately. We have presented a method to estimate the parameter ϵ. It remains to find an analytical formula to estimate an appropriate value of the parameter ϵ which best regularizes the heat conduction model. It is hoped that our method may motivate further research and suggest where it might be found.

Acknowledgment:

The authors wish to acknowledge support provided by the King Fahd University of Petroleum and Minerals.

References

[1] Heinz W. Engl, Martin Hanke and Andreas Neubauer, Regularization of Inverse Problems, Kluwer, Dordrecht, 1996, pp. 31-42.

[2] C. F. Weber, Analysis and solution of the ill-posed problem for the heat conduction problem, International Journal of Heat and Mass Transfer 24 (1981) 1783-1792.

[3] L. Elden, Inverse and Ill-Posed Problems, (H. W. Engl and C. W. Groetsch, eds.), Academic Press, Inc. 1987, pp. 345-350.

[4] Ali Vedavarz, Kunal Mitra and Sunil Kumar, Hyperbolic temperature profiles for laser surface interactions, J. Appl. Phys. 76(9) (1994) 5014-5021.

[5] U. Gratzke, P. D. Kapadia and J. Dowden, Heat conduction in high-speed laser welding, J. Phys. D: APPL. Phys. 24 (1991) 2125-2134.

[6] H. W. Wyld, Mathematical Methods for Physics, W. A. Benjamin, Inc., Massachusetts, 1976, pp 154-176.

[7] W. Walter, Ordinary Differential Equations, Springer-Verlag, New York, 1998, pp 70.

[8] C. M. Bender and S. A. Orszag, Advanced Mathematical Methods for Scientists and Engineers, McGraw Hill, New York, 1978.

[9] H. S. Carslaw and J. C. Jaeger, Conduction of Heat in Solids, Oxford University Press, 1959.

[10] P. C. Hansen, Rank-Deficient and Discrete Ill-Posed Problems. Numerical Aspects of Linear Inversion, SIAM, 1997.